DOI:10.16262/j.cnki.1005-0841.2004.z1.023

Electronic Characterization of the Single-wall CarbonNanotubes: A XANES Study

Wu Z.Y.[1] Hu T.D.[1] Terranova M.L.[2] Orlanducci S.[2] Sessa V.[2]
Abbas M.[1] Ibrahim K.[1] Zhong J.[1] Botti S.[3] Davoli I.[4]

(1 Beijing Synchrotron Radiation Facility, Institute of High Energy Physics, Beijing 100039;
2 Dip. di Scienze e Tecnologie Chimiche and INFM, Università di Roma "Tor Vergata", Italy;
3 ENEA, Divisione Fisica Applicata, P.O. Box 65, 00044 Frascati, Italy;
4 Dip. di Fisica and INFM, Università di Roma "Tor Vergata", Italy)

The single-wall carbon nanotubes (SWCNs) were discovered in '93[1] and are made of pure carbon atoms just like a single sheet of graphite wrapped around a cylindrical axis. The same material with slight variations in the geometrical arrangement yields different electronic properties, which could range from metallic to semiconducting behavior. They have fascinating chemical, mechanical and electrical properties which result remarkably different from those of any other carbon-based materials and which suggest enormous potential application in many technological areas, as catalysis, energy and gas storage, electron emitters, sensors, fast acting switches, molecular electronics, etc.[2-6]. In this contest it is very important to know and to control the electronical and chemical characteristics of the SWCNs.

Different methods were proposed to fabricate carbon nanotubes. The approach to the production of SWNTs in this work relies on metal-catalysed reactions between atomic H and C nanopowders[7]. The amorphous C nanoparticles (diameter 40 ± 20 nm) are prepared by cw-CO_2 laser-assisted pyrolysis of ethylene/acetylene mixtures in a flow-reactor[8]. The carbon nanotubes are generated using a CVD (Chemical Vapour Deposition) apparatus which connected to a powder-flowing system that is formed by a powder reservoir, a mass flow controller and a final Mo nozzle which can be translated and rotated around the longitudinal axis. A scheme of the apparatus can be found in the aticle[9]. The C nanopowders are swept from the reservoir by Ar streams, and homogeneously distributed by the nozzle, then they across the active area of the substrate where interaction with atomic H takes place. The main parameters of the synthesis process are: H_2 flowing rate 200 cm^3/s; Ar flowing rate 40-60 sm^3/s; substrate temperature 800—900°C. The produced nanotubes are deposited onto Si plates coated by a submicron dispersion of Fe particles. The samples investigated in this paper are representative of different kind or material which can be obtained by varying Ar flow rate and substrate temperature.

The analyses of structural and morphological characterization of the two kinds synthesized SWCNs are carried out using Raman spectroscopy, electron microscopy (SEM), and tunneling microscopy (STM).

The SEM micrographs of Fig.1 (a) and (b) show the morphology of two deposits formed by self-organized nanotubes joined together in bundles. The STM analysis has been performed on a scanning probe microscope Jeol JSPM-4210, which is in low-vacuum conditions, at tunneling currents in the range 0.100—0.300 nA and at biases in the range 0.100— 0.300 V. The STM image obtained from the same deposits is shown in Fig.2, that can be evidenced a bundle formed by single wall carbon nanotubes aligned on a nanometric scale. Further information about the observed nanostructures has been obtained by Raman analysis in the 80-400 cm^{-1} of the Radial Breathing Mode (RBM) spectral region. The spectra are taken at room temperature in the backscattering configuration using an Ar^- ion laser beam (wavelength: 514.5nm; laser power 10 mW; spectral resolution: $3cm^{-1}$). The analysis of the Raman spectrum taken in the RBM spectroscopic region shows that SWCNs are the dominant product under the catalytic growth conditions (Fig.3).

X-ray absorption spectroscopy (XAS) is a local technique of analysis based on the excitation of electronic transition from an inner level to outer unoccupied states. The photoabsorption process yields information on the local electronic structure and coordination envi-

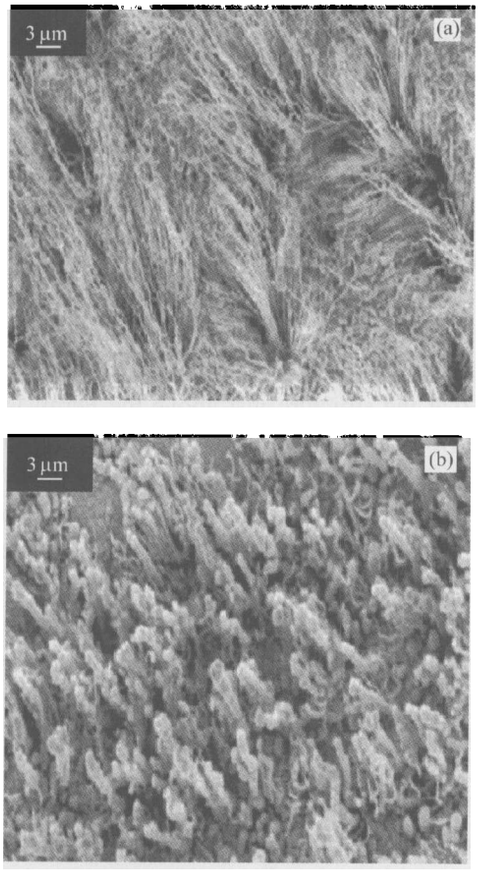

Fig.1 SEM image of SWCNs deposits:(a)sample 1;(b) sample 2.

ronment around the absorbing atom. XAS techniques such as EXAFS (Extended X-ray Absorption Fine Structure) and XANES (X-ray Absorption Near Edge Structure) have been used extensively to investigate the local structure in the interior and at the surface, as well as bonding formation of a variety of solid-state materials [10-12].

The experimental set-up for the investigation of absorption spectra at the C K-edge was described in the aticle[13]. Samples are loaded in an ultrahigh vacuum chamber and maintained in a background pressure of ~8×10^{-8} Pa, although during the data of acquisition the pressure rises up to ~1×10^{-7} Pa. The spectra are detected using the total electron yield (TEY) mode, i. e. a surface-sensitive detection method with a typical probing depth of a few nm. The photon energies used to record the C K-edge absorption spectrum range from 275 to 320 eV, and the experimental resolution at these photon energies is about 0.3 eV.

The C K-edge XANES spectra of the carbon nanotubes (samples1 and 2) in TEY are reported in Fig.4.

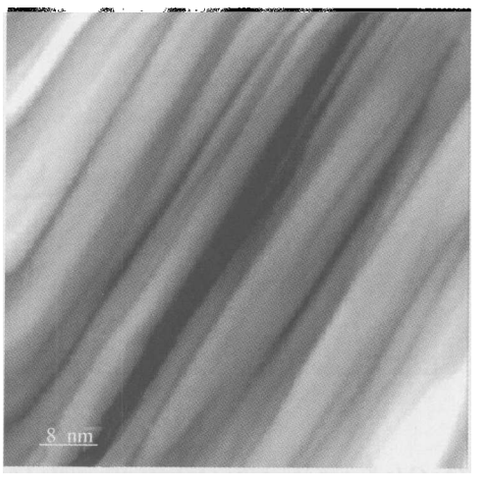

Fig.2 STM image showing the assembling of the nanotubes in a bundle.

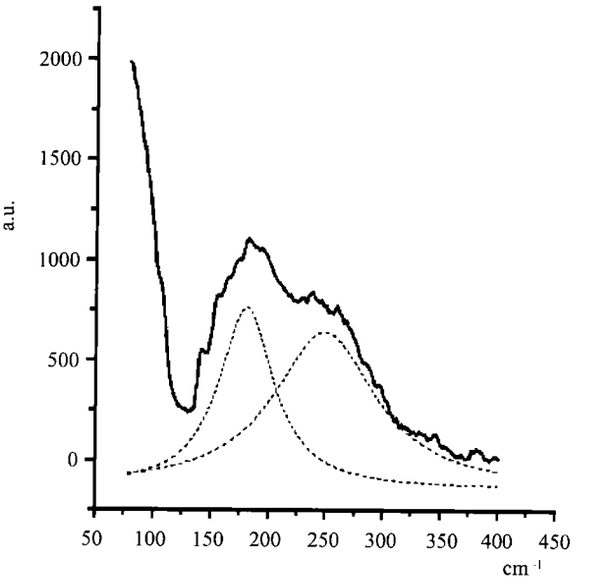

Fig.3 Raman spectrum in the RBM region of a typical sample.

According to the dipole-allowed transition selection rule, all spectral features are due to transitions from the carbon 1s core level to p-like final unoccupied states. The spectra show well-resolved transition features denoted as peaks A to D above the threshold. From previous work [14-19], the two prominent transition features A and C at 285.5 and 293 eV may be associated with the existence of unoccupied π^* and σ^* bands, respectively. The behavior of transition peaks in both spectra are quite similar indicating that the short-range environment in both samples has the same structure. The spectral features B may be an indication of the σ^* resonance characteristic of C-H bonds[20-22].

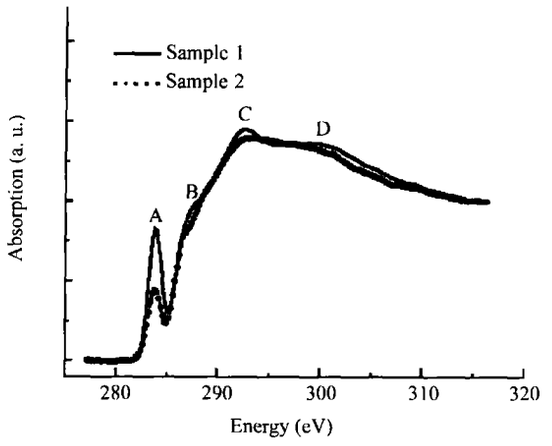

Fig.4 The C 1s X-ray absorption spectra of sample 1 and sample 2 in total electron yield.

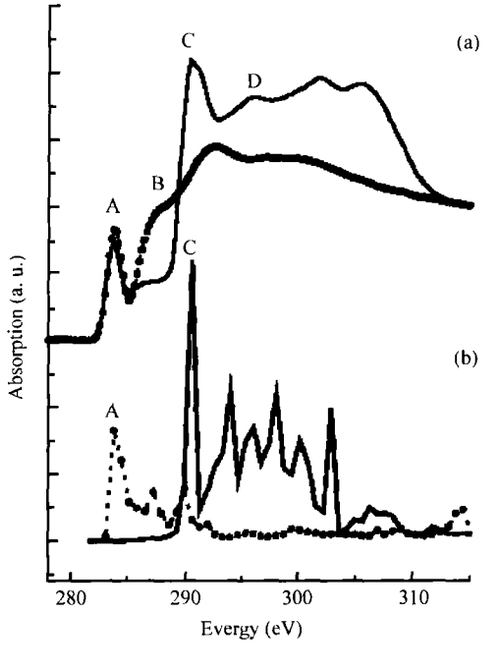

Fig.5 (a) Comparison of the C K-edge XANES spectra of sample 1 (dot line) and highly orientedpyrolytic graphite (HOPG) in TEY (panel a); (b) Polarized multiple-scattering calculations of the C K-edge XANES of graphite: Z-component (dot line) and XY-components (solid line).

From the spectrum it is evident that the peaks of sample 2 are smoother compared to those of sample 1, which implies that the "medium-range" structure of SWCNs of sample 2 is more distorted and/or amorphous on the surface.

In Fig. 5 (a) we present the comparison of the C K-edge XANES of sample 1 of SWCNs and the spectrum of highly oriented pyrolytic graphite (HOPG) in TEY. The latter spectrum exhibits a reasonable agreement with previous published data [14-18], i.e., the spectrum composed by three main features: an almost atomic contribution at about 285.5 eV, a peak at about 293 eV and the main large MS resonance centred at about 305 eV and labelled: A, C and D, respectively. The weak feature near 287.5 eV is generally observed in the x-ray absorption spectra of graphite and attributed to the free-electron-like interlayer states in the graphite [23,24]. If we look to the peak A, the intensity of this feature does not change significantly between CNT and HOPG, indicating that the structure just above the Fermi level is mainly a molecular interaction between the central atom and its nearest neighbour coordination shell (short-range effects), which addresses also a reasonable ordering of the carbon matrix. However, a difference between the spectra of SWCNs and HOPG can be recognized looking at the 289 -320 eV region: the transition $1s \rightarrow \sigma^*$ -like states is less intense and fairly broadened in the SWCNs. This behaviour implies that the "long- or medium-range" atomic order deviates from graphite one (e.g. disorder and/or distortion effects). Actually in a bundle of self assembled nanotubes, carbon atoms experience an anisotropic geometry due to the bonding with atom of the same tube or of the adjacent tubes. The anisotropic environment of the carbon atoms can be certainly one of the causes of the distortion of the original trigonal structure. This mechanism, in turn, increases the number of distinct photoelectron scattering paths in a nanotube, yielding a broadening of the XANES spectrum. These effects may be due to a random phase decoherence among each set of closely similar multiple scattering paths and the variation in the threshold E_0 in the absorption coefficient [25]. Such effects could be also ascribed to the fact that the tubes in the bundles are not infinitely long nor perfectly straight. However, also the compositional disorder, i.e. the presence of H atoms of others impurities, leads to the smearing of near-edge features.

In Fig. 5(b) for comparison we present the polarized XANES calculation of graphite using 215-atom cluster within a sphere of radius 7.5Å in the framework of the multiple scattering theory [26-30]. It is clearly evidenced in the dot line that the π^* states (peak A) are reproduced in the Z- polarized component which corresponds to C $2p_x$ and $2p_y$ orbitals. This resonance is the strongest at grazing x-ray incidence when the x-ray electric field vector has a large projection along the direction

of the p orbital, and it is the weakest at normal x-ray incidence when the electric field vector is perpendicular to the p orbital[19]. The corresponding 1s to σ^* transitions around 293 eV appears in the XY-polarized calculation which contains the C $2p_z$ orbital and exhibits the opposite trend as expected since the σ^* is orthogonal to the π^*. It is work to notice that the position of σ^* feature in SWCNs shifts towards higher energy that those in graphite indicating than the C-C distances in SWCNs are shorter than the one in graphite. The quantitative simulation are in progress and will be presented in a forthcoming paper.

In conclusion, it is possible to growth well aligned arrays of packed nanotubes using the reported synthesis approach, and they are confirmed also by SEM, STM images and Raman data. Moreover, the data at the C K edge in SWCNs and comparison with graphite show that structural and bonding configurations can be recognised looking at the characteristic pre-edge features. The investigation of the different features in the multiple-scattering region is of importance to better understand topology and ordered degree of these materials. The achieved results are also consistent with the expected chemical environment of carbon nanotubes.

Acknowledgements Wu Z.Y. acknowledges the financial support provided by the Major-Research Plane-Nanoscience and Technology Basic Research (90206032) and the Outstanding Youth scholars Fund (10125523) of the National Natural Science Foundation of China.

References

[1] Iijma S., Ichihashi T. Nature, 1993, 363: 603.

[2] Bockrath M., Cobden D. H., Lu J. et al. Nature, 1999, 397: 598.

[3] Yao Z., Postma H.W.J., Balents L. et al. Nature, 1999, 402: 273.

[4] Avouris P. Chem. Phys., 2002, 281: 429—445.

[5] Kasumov Yu. et al. Science, 1999, 284,1508; Kociak M.et al. Phys. Rev. Lett., 2001, 86, 2416.

[6] Inagaki M.New Carbons-Control of Structure and Functions. Elsevier Science, 2000.

[7] Terranova M.L., Piccirillo S., Sessa V.et al. Materials Chemistry and Physics, 2000, 874:1.

[8] Botti S., Coppola R., Gourilleau F. et al. J.Appl.Phys., 2000, 88: 3396.

[9] Terranova M. L., Piccirillo S., Sessa V. et al. Chem. Phys. Lett., 2000, 327: 284.

[10] Hamad K. S., Roth R., Rockenberger J.et al. Phys. Rev. Lett., 1999, 83: 3474.

[11] Rehr J.J., Albers R.C. Rev. Mod. Phys., 2000, 72: 621.

[12] Wu Z.Y., Zhang J., Ibrahim K. et al. Appl. Phys. Lett., 2002, 80: 2973.

[13] Liu F. Q., Ibrahim K. et al. J. Elect. Spectrosc. & Rel. Phenom., 1996, 80: 409.

[14] Weng X.D., Rez P., Ma H. Phys. Rev. 1989, B40: 4175.

[15] Bruhwiler P. A., Maxwell A. J., Puglia C. et al. Phys. Rev. Lett., 1995, 74: 614.

[16] Bruley J., Williams D. B., Cuomo J. J. et al. J. Microscopy, 1995, 180: 22.

[17] Tang Y.H., Zhang P., Kim P.S. et al. Appl. Phys. Lett., 2001, 79: 3773.

[18] Imamura M. et al. Physica, 1995, B208(209): 541.

[19] Tang Y. H., Sham T.K., Hu Y. F. et al. Chem. Phys. Lett., 2002, 366: 636—641.

[20] Stohr J.NEXAFS Spectroscopy (Springer, New York, 1992).

[21] Ishii I., Hitchcock A.P.J. Electron Spectrosc.Relat. Phenom., 1988, 46: 55.

[22] Wesner D., Krummacher S., Carr R. Phys. Rev., 1983, B28: 2152.

[23] Fischer D. A., Wentzcovitch R. M., Carr R. G. et al. Phys. Rev., 1991, B44: 1427.

[24] Pickard C. J., thesis Ph.D. Christ's College, 1997.

[25] Farges F., Brown G.E., Rehr J.J.Phys. Rev., 1997,B56: 1809.

[26] Lee P.A., Pendry J.B. Phys. Rev., 1975: B11: 2795.

[27] Natoli C.R., Benfatto M., Brouder C. et al. Phys. Rev., 1990, B42:1944; Tyson T.A., Hodgson K.O., Natoli C.R. et al. Phys. Rev., 1992, B46:5997.

[28] Durham P.J., Pendry J.B., Hodges C.H.Solid State Commun., 1981, 38: 159; Comput. Phys. Comm., 1982, 25: 193.

[29] Vvedensky D. D., Saldin D.K., Pendry J .B. Comput. Phys. Commun., 1986, 40: 421.

[30] Durham P. J. in X-ray Absorption: Principles, Applications, Techniques of EXAFS, SEXAFS, XANES, edited by Prinz R. and Koningsberger D. (Wiley, New York, 1988).